

Line flux measurement of infrared galaxies in the *AKARI* NEP field with Keck/DEIMOS

AYANO SHOGAKI,¹ SHUJI MATSUURA,¹ NAGISA OI,² TOMOTSUGU GOTO,³ HIDEO MATSUHARA,⁴ KAZUMI MURATA,⁴
TOSHINOBU TAKAGI,⁵ TAKUYA OTSUKA,⁶ MATTHEW MALKAN,⁷ AND SAYAKA CHUREI⁴

¹*Kwansei Gakuin University, 2-1 Gakuen, Sanda, Hyogo 669-1337, Japan*

²*Tokyo University of Science, 1-3 Kagurazaka, Shinjuku-ku, Tokyo 162-8601, Japan*

³*Institute of Astronomy and Department of Physics, National Tsing Hua University, No. 101, Section 2, Kuang-Fu Road, Hsinchu, Taiwan 30013, R.O.C*

⁴*Institute of Space and Astronautical Science, Japan Aerospace Exploration Agency, 3-1-1 Yoshinodai, Chuo, Sagami-hara, Kanagawa 252-5210, Japan*

⁵*Japan Space Forum, Shin-Ochanomizu Urban Trinity Bldg. 2F, 3-2-1, Kandasurugadai, Chiyoda-ku, Tokyo 101-0062 Japan*

⁶*Astronomical Institute, Tohoku University, 6-3, Aramaki, Aoba-ku, Sendai, Miyagi, 980-8578, Japan*

⁷*UCLA Physics & Astronomy, 475 Portola Plaza, Los Angeles, CA 90095-1547, USA*

ABSTRACT

We analyzed 553 spectra of infrared sources in the *AKARI* NEP deep field observed with Keck/DEIMOS in 2011. In previous work, we conducted a spectroscopic diagnostics of the sources based on relative line fluxes without the absolute flux calibration, and the analysis was not done for all detected sources due to a technical reason. In this work, we present a preliminary report on measurement of absolute line flux for all detected sources. For the flux calibration of the DEIMOS spectra, we adopted the photometric (*r*- or *i*-band) flux to determine the scaling factor of the average flux in the blue or red channel of DEIMOS. As a result of our analysis, we obtained emission spectra of 304 galaxies showing hydrogen recombination lines and forbidden lines of heavy elements, e.g., [O III] line.

Keywords: techniques: spectroscopic, methods: data analysis, catalogs, infrared: galaxies, galaxies: star formation, galaxies: evolution

1. INTRODUCTION

The *AKARI* North Ecliptic Pole (NEP) deep field was chosen as core survey field dedicated for multi-wavelength study of distant infrared galaxies (Krumpe et al. 2015; Shim et al. 2013). For spectroscopic diagnostics and redshift determination of the infrared galaxies, 550 samples from a preliminary *AKARI* NEP Deep source catalog (Wada et al. 2008; Takagi et al. 2012) were observed with Keck/DEIMOS in 2011. In previous analysis of the DEIMOS data, spectroscopic diagnostics of star-forming galaxies using relative intensities of coronal lines was attempted, but absolute flux information has been demanded for further study of physical property and evolutionary track of infrared galaxies. In this work, we calibrated absolute fluxes of the DEIMOS spectra by scaling with photometric flux from the latest optical-NIR source catalog in the *AKARI* NEP Deep field (Oi et al. 2014).

2. DATA REDUCTION & FLUX CALIBRATION

2.1. Rawdata pipeline

We used the DEEP2 DEIMOS reduction pipeline (<http://www2.keck.hawaii.edu/inst/deimos/pipeline.html>) for analyzing DEIMOS raw data. The code does a job of wavelength fitting, sky subtraction, and object fitting and outputs all of the 2-d slit spectra (flux as a function of wavelength) stacked in an image and aligned in wavelength space. Finally, we obtain 1-d spectra as ADU values from each of the slit through 2-d spectra tracing process.

2.2. Relative Flux Measurement

In previous analysis with the standard pipeline, we found some deficits in the standard star spectra due to an error in the source line tracing process on the 2-d spectral image. Thus, we re-processed the standard star data by using our own

source tracing code, and computed an improved spectral response curve from average spectra of two standards.

$$\text{response curve} = \frac{\text{standard star flux} [\text{erg cm}^{-2} \text{s}^{-1} \text{\AA}^{-1}]}{\text{standard star spectra by DEIMOS} [\text{ADU}]}$$

Using the response curve, we converted raw spectra of observed galaxies in ADU to spectral fluxes in $\text{erg cm}^{-2} \text{s}^{-1} \text{\AA}^{-1}$ as (DEIMOS spectra [ADU]) \times (response curve). Finally, we corrected the measured spectra for airmass according to Mauna Kea summit extinction values.

2.3. Absolute Flux Measurement

Since absolute flux of measured spectrum is usually lower than actual source flux due to coupling loss to slit, we corrected the measured spectrum by scaling to the measured photometric flux from the optical-NIR multi-band source catalog (Oi et al. 2014). We first computed flux correction factor for each source in the short- and long-wave range of the DEIMOS spectrum as the ratio of the integrated spectrum in 5500–7300 \AA and 6800–8700 \AA to the r - and i -band photometric flux, respectively,

$$r, i \text{ flux correction factor} = \frac{\text{Averaged flux of galaxy spectra@r-,i-band}}{\text{Photometry flux@r-,i-band}}.$$

We finally used common flux correction factor for all sources as average value for the sources with signal-to-noise ratio (SNR) > 10 , because flux correction for the low-SNR sources could increase the absolute flux error. Resultant flux correction error is estimated to 8% and 10% for the short- and long-wave range, respectively.

In Figure 1, we present typically measured spectra of line-emitting galaxies after flux calibration.

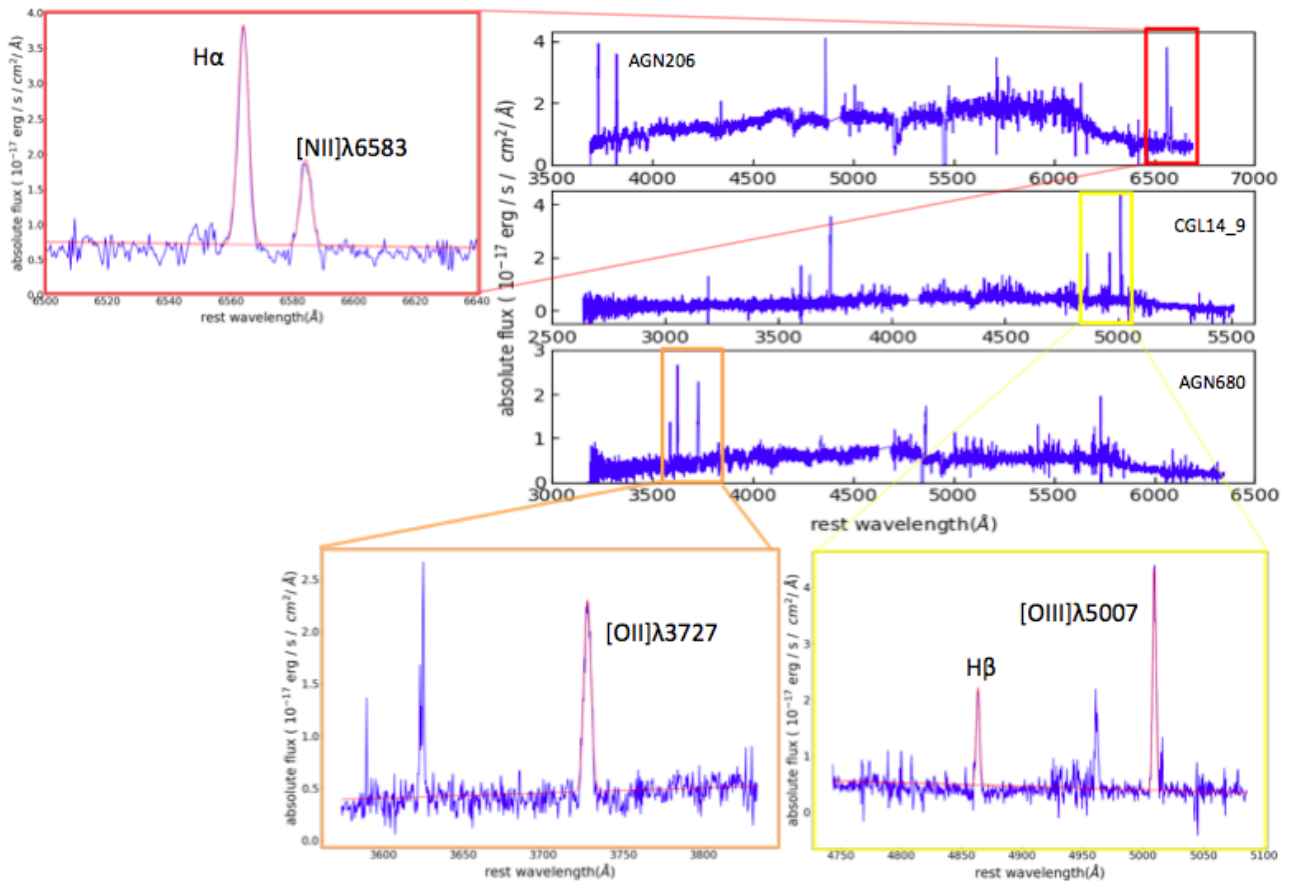


Figure 1. Typical spectra of the DEIMOS sources after flux calibration with magnified view of emission lines; H-recombination lines and forbidden lines.

3. STATISTICS OF DETECTED SOURCES

Breakdown of detected sources is summarized in Table 1. Compared with previous analysis, additional 3 sources were newly detected by this analysis.

Table 1. Source breakdown

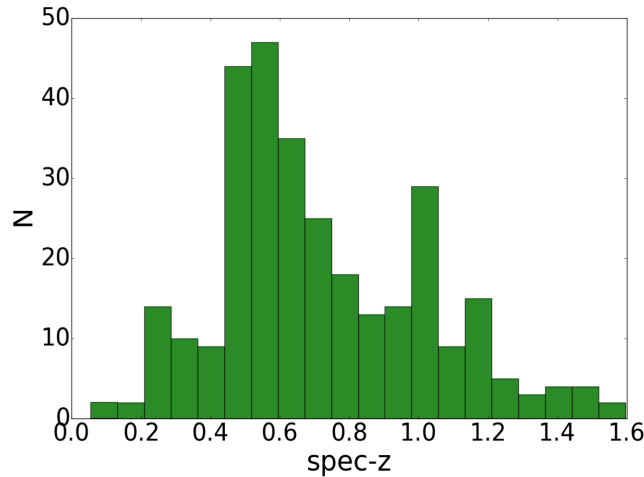
| Detail | Number of sources |
|--|-------------------|
| Total targets | 570 |
| Detected | 553 |
| Matched with <i>AKARI</i> catalog (Oi et al. 2014; Murata et al. 2013) | 546 |
| Emission-line galaxies | 304 |

We identified emission lines by pattern matching of line spacings in wavelength by eyes. In the case that any absorption line is not identified and only single line is detected, we identified the line to be [O II] line with confirmation of photometric redshift. In order to measure center wavelength, line width, and intensity of emission line, we fitted the measured spectral profile with single- or double-Gaussian function(s) as a function of wavelength x ;

$$g(x) = A \times \exp \frac{-(x-d)^2}{2\sigma^2} + px + q,$$

where A is the amplitude, d is the center wavelength, and σ is the standard deviation. The linear term $px+q$ fits the continuum around the line. We calculated the total line flux by integrating the best-fit Gaussian function in wavelength. We also measured spectroscopic redshift (z_{spec}) from the center wavelength of [O II] line. If [O II] line is not detected but another emission-lines are measured by gaussian, we used most luminous line for redshift determination.

Figure 3 shows redshift distribution of the detected sources.

**Figure 2.** Spectral redshift distribution of DEIMOS emission-line sources.

4. EMISSION-LINE SOURCE PROPERTIES

4.1. [O II] Luminosity

To investigate the star formation activity of our 256 line emitting galaxy samples, we measured the extinction-uncorrected [O II] luminosity from the measured line flux.

$$L_{[\text{O II}]} = 4\pi d_L^2 \times \text{line flux} [\text{erg s}^{-1} \text{cm}^{-2}] = \frac{4\pi d_L^2 \times \text{line flux}}{3.826 \times 10^{33}} [L_{\odot}],$$

where d_L is the luminosity distance calculated from spectroscopic redshift for a cosmology with $([h, \Omega_m]) = (0.72, 0.3)$. Fig.3 shows the [O II] luminosities of our samples as a function of z_{spec} , which accords to well-known behavior of star formation rate (SFR) increasing with redshift.

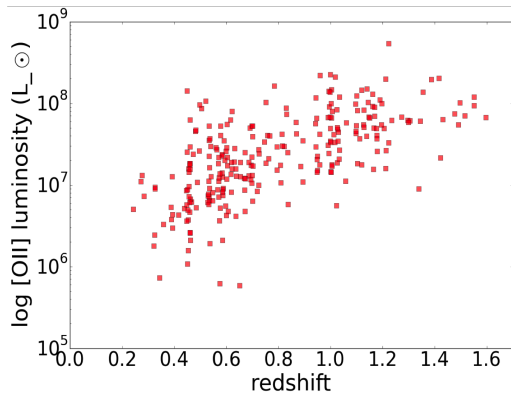
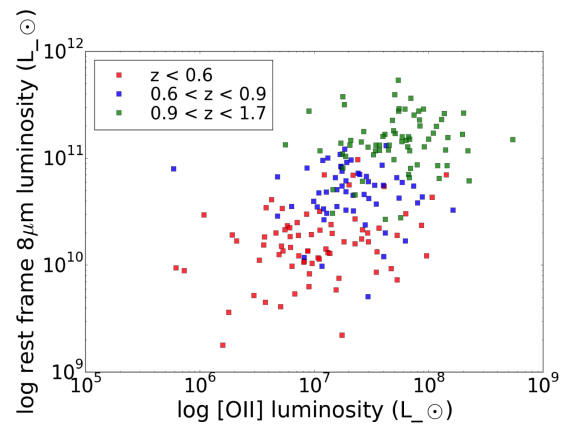
4.2. Rest-Frame 8 μm Luminosity

It is known that the 8 μm luminosity of star forming galaxy can well represent total infrared luminosity, which is a reliable indicator of SFR. We compared the SFR from the [O II] luminosity with the SFR from the rest-frame 8 μm luminosity from the *AKARI* multi-band photometry data (Murata et al. 2013).

For a glance of correlation between the [O II] line and the infrared luminosity, we used the *AKARI* photometric flux in different filter band (*S11*, *L15*, and *L18W*) depending on redshift to obtain the rest-frame 8 μm luminosity without the K-correction (Goto et al. 2010). Redshift bins and corresponding *AKARI* filters for the analysis are listed in Table 2. In Figure 4, we show the correlation between the [O II] luminosity and the rest-frame 8 μm luminosity. There seems to be systematic increase of the 8 μm /[O II] ratio with increasing redshift.

Table 2. Redshift bins

| Redshift | <i>AKARI</i> filter |
|-----------------|---------------------|
| $z < 0.6$ | <i>S11</i> |
| $0.6 < z < 0.9$ | <i>L15</i> |
| $0.9 < z < 1.7$ | <i>L18W</i> |

**Figure 3.** [O II] luminosity distributions as redshift**Figure 4.** [O II] luminosity vs 8 μm luminosity relation

5. SUMMARY

We reported revised process of spectroscopic data taken with Keck/DEIMOS in the *AKARI* NEP Deep field. In this work, we obtained absolute spectral flux with higher accuracy than previous work. We demonstrated that this new spectroscopic data set would be useful for detailed study of infrared galaxies, for example, by showing evolution of the SFR from the [O II] luminosity, and the correlation between the [O II] line and infrared luminosity.

REFERENCES

- Goto, T., Takagi, T., Matsuhara, H., et al. 2010, *A&A*, 566, A60
 Krumpe, M., Miyaji, T., Brunner, H., et al. 2015, *MNRAS*, 446, 911
 Murata, K., Matsuhara, H., Wada, T., et al. 2013, *A&A*, 559, A132
 Oi, N., Matsuhara, H., Murata, K., et al. 2014, *A&A*, 566, A60
 Shim, H., Im, M., Ko, J., et al. 2013, *ApJ*, 207, 37
 Takagi, T., Matsuhara, H., Goto, T., et al. 2012, *A&A*, 537, A24
 Wada, T., Matsuhara, H., Oyabu, S., et al. 2008, *PASJ*, 60, S517